Chemical Physics Letters 464 (2008) 181–186

Contents lists available at ScienceDirect

Chemical Physics Letters

journal homepage: www.elsevier.com/locate/cplett

Spectroscopic and photophysical properties of salicylaldehyde azine (SAA) as a photochromic Schiff base suitable for heterogeneous studies

Marcin Ziółek [a,c,*], Katarzyna Filipczak [b], Andrzej Maciejewski [b,c]

[a] Quantum Electronics Laboratory, Faculty of Physics, Adam Mickiewicz University, Umultowska 85, 61-614 Poznan, Poland
[b] Photochemistry Laboratory, Faculty of Chemistry, Adam Mickiewicz University, Grunwaldzka 6, 60-780 Poznan, Poland
[c] Center for Ultrafast Laser Spectroscopy, Adam Mickiewicz University, Umultowska 85, 61-614 Poznan, Poland

ARTICLE INFO

Article history:
Received 9 May 2008
In final form 15 September 2008
Available online 19 September 2008

ABSTRACT

The photochromic cycle of the salicylaldehyde azine (SAA) has been investigated by means of the stationary and time-resolved UV–vis spectroscopy in a number of differently interacting solvents and micellar systems. The primary enol form of this Schiff base is much more energetically stabilized than in the other aromatic Schiff bases, which is reflected in remarkable resistance of SAA to the hydrolysis process. The fluorescence decay measured in highly viscous solvents as well as in micellar systems has proved the existence of different conformers of the *cis*-keto tautomer. Three different routes of the photochrome (*trans*-keto tautomer) decay have been also observed.

1. Introduction

The best known photochromic Schiff base, salicylideneaniline (SA), as well as the related compounds for many decades attracted much interest [1–9] and nowadays are widely studied because of possible applications, e.g. in molecular memories and switches [10,11]. The salicylaldehyde azine (SAA), see Fig. 1, is the smallest possible symmetric aromatic Schiff base (with two hydrogen-bonding centres) belonging to the 'SA family'.

According to our knowledge, there are only a few reports on SAA properties in solid state [12–15]. The SAA molecules are nearly planar with strong intramolecular hydrogen bonds and are packed in the plane-to-plane stacks within the crystal, which accounts for its thermochromic properties [12,13]. Even fewer reports have been published on SAA properties in solution [16–18] in which state it reveals the photochromic behaviour (like all other Schiff bases). In acetonitrile solution, the lifetime of the ground state of the photochrome (*trans*-keto tautomer) was found to be nearly two orders of magnitude shorter than that for the other aromatic Schiff bases [17].

Recently, we have reported the studies of SAA in femto- and picosecond time domains in the same solvent and found that the results are very similar to those obtained for SA [18]. After the excitation of the enol form (Fig. 1) to the first singlet state S_1 (π,π^*) an ultrafast excited state intramolecular proton transfer reaction takes place with the characteristic time below 50 fs [18]. As a result, a *cis*-keto tautomer (Fig. 1) in S_1 (π,π^*) state is created exhibiting a characteristic, strongly Stokes shifted, fluorescence. It has been concluded that despite the two possible proton transfer centres, the excitation of symmetric Schiff bases in solution is localized on one salicylidene subunit and the single proton transfer occurs [3,4,17]. Also, the semi-empirical calculations for SAA predict the excited state single proton transfer rather than the double one [15]. Therefore, for simplicity, the excited SAA monoketo-tautomer will be called 'keto' throughout the article. The lifetime of the S_1 (π,π^*) state of SAA *cis*-keto tautomer equals 19 ps in acetonitrile [18]. Finally, after the structural changes in this tautomer (involving the cleavage of the intramolecular hydrogen bond) about 20 ± 10% of excited molecules are transferred to the long-lived ground state of the photochromic form (probably *trans*-keto tautomer, see Fig. 1) [18].

In this Letter, we present and discuss the solvatochromic measurements of the spectroscopic and photophysical properties of all the SAA tautomers in 15 differently interacting homogeneous solvents and three different micro-heterogeneous micellar systems, performed by means of the stationary and time-resolved UV–vis spectroscopy. In the three parts of Section 3, the properties of the enol, *cis*-keto and photochrome (*trans*-keto) tautomer are investigated.

2. Experimental

SAA was synthesized by condensation of hydrazine with salicylaldehyde and was recrystallized from ACN. The solvents used were the same as in our previous paper [19], their abbreviations are given in Table 1 and their solvatochromic parameters (Kamlet-Taft [20] and Catalán [21] scale) are presented in Table S1 (in Supplementary material). The concentration of SAA was between

* Corresponding author. Address: Quantum Electronics Laboratory, Faculty of Physics, Adam Mickiewicz University, Umultowska 85, 61-614 Poznan, Poland.
E-mail address: marziol@amu.edu.pl (M. Ziółek).

0009-2614/$ - see front matter © 2008 Elsevier B.V. All rights reserved.
doi:10.1016/j.cplett.2008.09.030

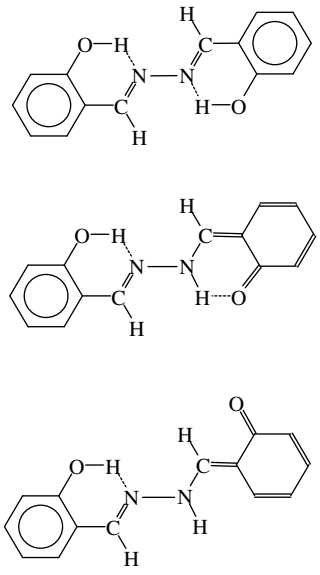

Fig. 1. Formula of SAA and its transient tautomeric forms. From up to down: enol, *cis*-keto and *trans*-keto (photochrome) tautomers.

1×10^{-5} and 1×10^{-4} M. In this range no changes in the absorption and emission spectra as well as in the fluorescence quantum yields were observed (checked in HEX and HEXD). Cetyltrimethylammonium bromide (CTAB, Fluka), Triton-X 100 (TX, Aldrich) and sodium dodecyl sulphate (SDS, Aldrich) were used as micelle forming surfactants. CTAB forms cationic, SDS anionic and TX non-ionic micelles in aqueous solutions. The concentration of the surfactants in water (purified and deionised) was 0.15 M. The maximum concentration of SAA in the micellar solution (reached after several hours of stirring) was about 1×10^{-4} M. Taking into account that SAA is almost insoluble in water (<2×10^{-7} M) it can be safely assumed that all of the SAA molecules are inside the micelles and not more than one SAA molecule per micelle is present in the above conditions [22,23] (see also the calculations in the Supplementary material).

The equipment for stationary and time-resolved measurements was the same as described in our previous papers [18,19,24]. The stationary UV–vis absorption spectra were measured with a UV–VIS-550 (Jasco) spectrophotometer and fluorescence emission spectra were recorded with a modified SPF-500 (Aminco–Bowman) spectrofluorimeter. The time-resolved emission measurements (time correlated single photon counting) were carried out at the magic angle and the pump wavelength was 380 nm (Ti: Sapphire laser). The pump pulse wavelength in the nanosecond transient absorption set-up was 355 nm (Q-switched Nd:YAG laser), the pump pulse energy was about 1 mJ and the kinetics were recorded in the spectral range 300–600 nm for every 25 nm. All measurements were performed at room temperature.

3. Results and discussion

3.1. Enol tautomer

The stationary absorption spectrum, in particular the long wavelength maximum at around 360 nm, originating from the transition $S_1 \leftarrow S_0$ (π,π^*) of the primary enol form is very similar for all solvents except the most protic ones (TFE and HFIP), see Fig. 2 and Table 1. Although the correlation with the solvatochromic scales is not very good (Table S2) the fit to Kamlet-Taft or Catalán scales reflects the main dependence of the maximum on different kinds of solvent interactions. Increasing the polarity of the solvent results in a slight blue shift, the proton accepting properties (in terms of hydrogen-bonding ability) have no influence on the maximum, while the proton donating abilities of the strong alcohols cause a relatively significant blue shift, see Fig. 2a. An increase in the solvent polarity as well as proticity results also in a greater absorbance at the minimum near 320 nm (Fig. 2a). The slight red shift of the maximum with increasing refractive index (and thus the polarizability function) for non-polar hydrocarbons (Table 1 and Fig. S1) is probably a manifestation of the role of dispersion interactions. It should be noted that the SAA cation measured in TFA has a much different absorption spectrum (Fig. S2) with the maximum at around 400 nm and, therefore, the blue shift of the absorption maximum in TFE and HFIP is certainly not due to the protonation of SAA. Moreover, the SAA anion measured in

Table 1
Photophysical properties of SAA in different solvents: maximum of stationary absorption (λ_{max}), maximum of stationary emission (ν_{max}), fluorescence quantum yield (φ_F), fluorescence lifetime (τ) and radiative rate constant (k_R)

Solvent	Absorption λ_{max} (nm) (±1 nm)	Emission ν_{max} (cm^{-1}) (exc. 360 nm) (±100 cm^{-1})	φ_F ($\times 10^{-3}$) (exc. 360 nm) (±20%)	τ (ps)[a] (exc. 380 nm) (±2 ps)	$k_R = \varphi_F/\tau$ ($\times 10^7$ s^{-1})
n-Hexane (HEX)	361	17 300	2.3	76	3.0
Nonane (NON)	362	17 200	3.7		
Hexadecane (HEXD)	363	17 200	4.5	130	3.5
Squalane (Sq)	363	17 150	3.9	140[b]	
1-Chloropropane (ClP)	359	17 100	1.6	50	3.2
Acetonitrile (ACN)	355	17 000	0.7	19	3.7
Ethanol (EtOH)	356	17 250	0.6		
Methanol (MeOH)	355	17 450	0.7	17	4.1
Ethylene glycol (EG)	357	17 100	2.6	76[b]	
Trifluoroethanol (TFE)	350	17 450	1.6	47	3.4
Hexafluoroisopropanol (HFIP)	345	17 500	2.7	67	4.0
Diethyl ether (DEE)	358	17 000	1.1		
Triethylamine (TEA)	359	17 350	2.1		
TX micelle	360	17 300	4.5	200[b]	
SDS micelle	357	17 250	2.7	110[b]	
CTAB micelle	360	17 200	6.2	240[b]	
NaOH in water	404	18 500	5.6		
Trifluoroacetic acid (TFA)	398				

[a] The fitting quality $\chi^2 < 1.2$.
[b] Average from multicomponent fit: $\langle\tau\rangle = \sum A_i\tau_i / \sum A_i$ (A_i is the amplitude of *i*th component of time constant τ_i), for the detailed data, see Table 2.

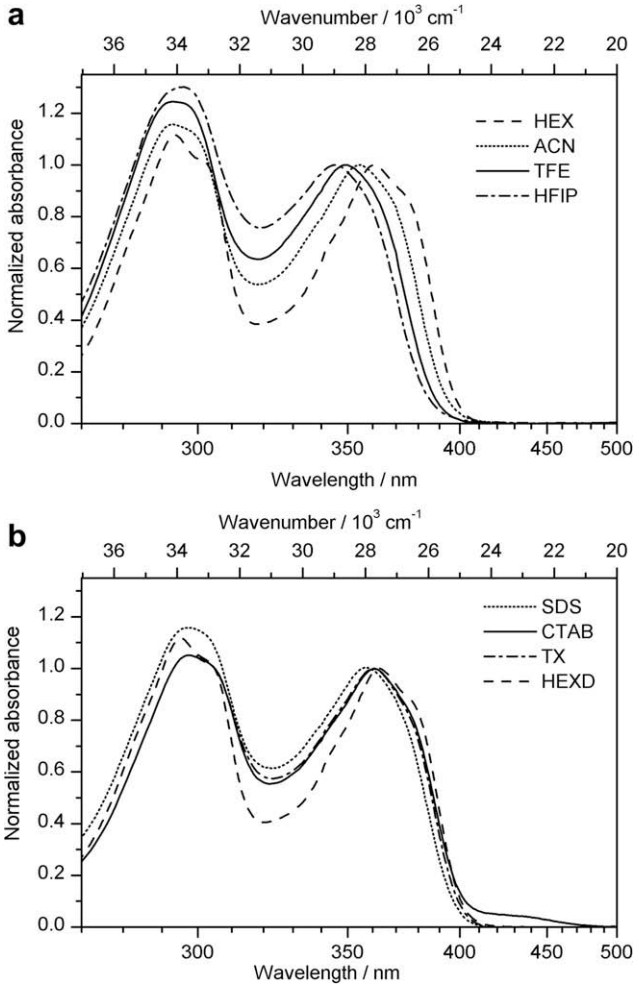

Fig. 2. Stationary absorption spectra of SAA in homogeneous solvent (a) and micellar solutions (b). The spectrum in HEXD is also added to (b) to show the differences between the spectrum in micelles and hydrocarbons.

NaOH (5×10^{-3} M) solution in water has the absorption spectrum similar to that of the cation. Thus, despite the strong basicity of TEA, no anion is formed in this solvent (Fig. S2).

In the absorption spectra of the other photochromic Schiff bases an additional long-wavelength band was observed in protic solvents (its intensity increased with the solvent proticity) ascribed to the $S_1 \leftarrow S_0$ (π,π^*) transition of the *cis*-keto tautomer stabilized by intermolecular hydrogen bond with the solvent [19,24]. For SAA, however, no indication of such a band is found even in HFIP, which means that the energy of the enol tautomer is much lower than that of the *cis*-keto tautomer and any enol-keto equilibrium in the ground state cannot be formed. The probable explanation of this fact is the presence of a stronger intramolecular hydrogen bond in the enol form of SAA, following from the enhanced basicity of the nitrogen atom, due to the absence of the conjugation with the aromatic ring bound to it [25]. It is our first evidence that the SAA enol form in solution is much more energetically stabilized than the other photochromic Schiff bases.

It is a known problem for Schiff bases that even small impurities of water can cause the process of their hydrolysis in protic environment [19,26,27]. For example, the water attack on the SA molecule causes its decomposition into salicylaldehyde and aniline [27]. We have measured the temporal absorption changes for the photochromic Schiff bases (studied by us previously [18,19,24]) in the H_2O:MeOH mixtures (volume ratio 1:4) and have found that only for SAA the hydrolysis process does not occur (see Figs. S3 and S4). This confirms the stability of the SAA enol form and makes this molecule a very good candidate for studying the photochromic Schiff bases in micro-heterogeneous micellar systems (formed in aqueous solution) as well as in mesoporous and microporous materials in which the traces of water are often hard to remove.

Having in mind this remarkable feature of SAA we performed its studies in water solutions of micelle forming surfactants. The stationary absorption spectra of SAA in TX, CTAB and SDS, presented in Fig. 2b, are similar to that in homogeneous solutions (note that in TX the surfactant absorbs up to 320 nm) and the shape of the absorption spectrum indicates that the SAA molecules are located in the polar part of the micelles. In the spectrum of CTAB additional long-wavelength band occurs. The profile of this band is close to the absorption spectra of SAA cation and anion and, thus, its probable explanation is the ion formation due to the interaction of the SAA molecules with CTAB or even acid or basic impurities.

3.2. *cis*-keto tautomer

Due to the ultrafast proton transfer reaction [18] the short-wavelength emission of the primary enol form is very weak and only the long-wavelength fluorescence with a maximum around 560–580 nm originating from the *cis*-keto tautomer was investigated in this study. The spectral position of the *cis*-keto stationary emission is nearly the same for all solvents, while the fluorescence quantum yield varies within one order of magnitude, see Table 1. The maximum of the emission spectrum is red shifted in polar non-protic solvents, and in these solvents the smallest fluorescence quantum yield is observed. Changing the environment to both the non-polar and more protic ones results in an increase in the quantum yield and a small blue shift of the fluorescence profile (Figs. S5 and S6). In hydrocarbons the fluorescence quantum yield increases with increasing polarizability function and/or viscosity of the solvent. Like we previously reported for SAA in ACN [18], the fluorescence excitation spectra measured in all other solvents at the *cis*-keto emission match the long-wavelength part of the $S_1 \leftarrow S_0$ (π,π^*) enol tautomer absorption spectrum (see Fig. S7).

The fluorescence decay in all homogeneous solvents studied except Sq and EG is mono-exponential and the lifetime varying from 17 to 130 ps is consistent with the fluorescence quantum yield (within the limit of its determination). The average radiative rate constant for all solvents equals $(3.5 \pm 0.5) \times 10^7$ s^{-1}. However, in much more viscous non-polar (Sq) and polar (EG) solvents the sufficient quality of the fit can be obtained only assuming that the fluorescence decay is two-exponential (Table 2). It should be noted that two-exponential decay was also observed previously for SA in polar and viscous cyclohexanol [2,8].

As presented in Table 2, we have also found two- or even three-exponential fluorescence decays for SAA in micellar systems. The shortest component of about 60 ps is similar in TX, SDS and CTAB, while the duration of the longer one significantly changes for different surfactants. The contribution of the short component slightly decreases with increasing wavelength. As evidenced in the stationary absorption spectrum (see Fig. 2) the shortest lifetime observed in SDS can be rationalized by the presence of SAA molecules in a more polar micro-environment in this micellar system than in TX and CTAB. The multi-exponential fluorescence decay observed in micelles and high-viscous solvents can be rationalized by the existence of at least two conformers of *cis*-keto tautomer which have similar $S_1 \leftarrow S_0$ (π,π^*) emission spectra. Some details of the justification of this hypothesis are presented in the Supplementary material.

It is most likely that the origin of the third and the longest fluorescence decay component of duration of about 1.5 ns observed in CTAB is different. The contribution of its amplitude decreases with

Table 2
Parameters (amplitudes a_i and lifetimes τ_i) of multi-exponential fit of SAA fluorescence in high viscous solvents and micellar systems

Solvent/ micelle	Emission wavelength (nm)	τ_1 (ps) (±10 ps)	a_1	τ_2 (ps) (±20 ps)	a_2	τ_3 (ps) (±100 ps)	a_3
Sq	550	90	0.29	160	0.71	–	–
	575	90	0.29	160	0.71	–	–
	600	90	0.28	160	0.72	–	–
EG	550	60	0.66	110	0.34	–	–
	575	60	0.65	110	0.35	–	–
	600	60	0.65	110	0.35	–	–
TX	550	60	0.33	230	0.58	500	0.09
	600	60	0.29	230	0.62	500	0.09
SDS	525	60	0.64	160	0.36	–	–
	550	60	0.57	160	0.43	–	–
	575	60	0.54	160	0.46	–	–
	600	60	0.51	160	0.49	–	–
CTAB	525	60	0.54	320	0.41	1500	0.05
	550	60	0.49	320	0.48	1500	0.04
	575	60	0.46	320	0.51	1500	0.03
	600	60	0.45	320	0.53	1500	0.02

The amplitudes are normalized to 1.

increasing wavelength. Thus, this decay component should be probably assigned to the emission of SAA ion which is present in CTAB (see previous section) and its fluorescence band is significantly blue shifted with respect to SAA *cis*-keto tautomer, see Table 1, Figs. S6 and S8.

3.3. trans-Keto tautomer

The transient absorption studies of the SAA photochrome (*trans*-keto tautomer) in the nano- and microsecond time scale were performed in HEX, ACN, MeOH, TFE, HFIP and the solutions of three micelle forming surfactants. The shape of the transient absorption spectra is similar in all solvents (a positive band with a maximum at around 475 nm assigned to the absorption from the S_0 state of the *trans*-keto tautomer and a negative band below 400 nm due to the ground state depopulation of the initial enol tautomer, see Fig. 3) while the transient decay and ground state

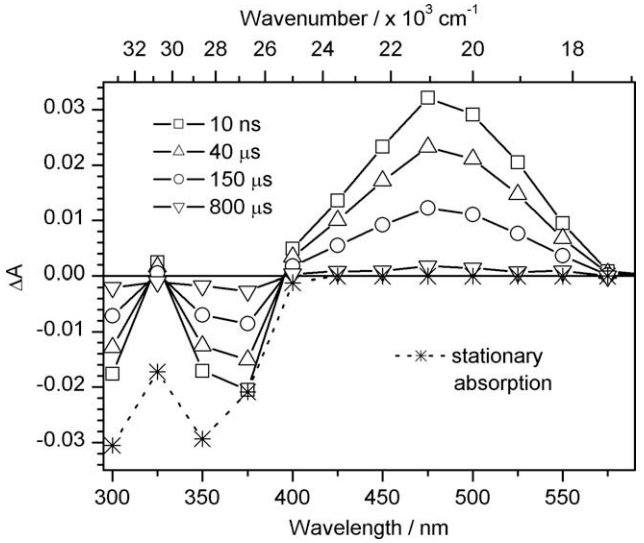

Fig. 3. Transient absorption of SAA in ACN ($c = 5 \times 10^{-5}$ M) for selected time delays. The stationary absorption spectra normalized to the measured initial depopulation bands are also shown.

recovery time constants differ by three orders of magnitude. No effect of oxygen was observed (checked in ACN) which means that the transient absorption from the triplet state does not contribute to the signals measured. The *trans*-keto tautomer lifetimes are generally about 10 times smaller than that of the other photochromic Schiff bases in the same solvents [4,6,7,19]. Significant residual negative signals of the depopulation band were frequently observed for the Schiff bases and explained by the *anti–syn* isomerisation within the enol form competing with the photochromic cycle [5,7,19] while in SAA the final transient absorbance of the ground state recovery represents no more than 10% of the initial transient absorbance in all solvents. Thus, the *anti–syn* isomerisation (around the N=C bond) of the enol tautomer plays a minor role in the deactivation scheme. These two facts (faster decay and small residual signals) confirm that the ground state of initial enol form (*anti*-enol) is more stable relative to the other tautomers, than in the other aromatic Schiff bases studied so far.

The decay pattern of the transient absorption of SAA was investigated by fitting a model function to the experimental data at particular wavelengths and in a global multi-exponential analysis approach. For SAA in the concentration of 5×10^{-5} M the half-lives are 8 μs in HEX and 95 μs in ACN, which reflects greater stabilization of the *trans*-keto tautomer in polar solvents [6,7]. In both solvents at a constant pump intensity, the lifetime increases in less concentrated solutions. This can be rationalized by the deactivation process that involves the complex of two SAA molecules in the *trans*-keto tautomer and, similarly as for related systems [6,28,29] the second-order double proton transfer reenolization can be proposed, see Fig. S14.

However, both pure first-order as well as pure second-order models (exponential and reciprocal functions, respectively, see Eqs. (S4) and (S5) in the Supplementary material) fail to adequately depict the kinetics measured in HEX and ACN. Therefore, a mixed first and second order case was assumed and then the kinetics can be expressed as follows [30]:

$$\Delta A(t) = A\,\frac{1-m}{e^{k_1 t} - m} + A_0, \qquad (1)$$

where A and A_0 denote the amplitudes of the decay and the constant offset signal, k_1 denotes the first-order rate constant (rate-determining back *trans–cis* isomerisation), $m = 2c_P k_2/(k_1 + 2c_P k_2)$ is the shape parameter ($m = 1$ for pure second-order reaction and $m = 0$ for pure first-order reaction), c_P is the concentration of the *trans*-keto tautomer and k_2 is the second-order rate constant. Eq. (1) very well describes the kinetics observed for ACN (Fig. 4). The triplet state of benzophenone [31] was used as the reference for the calculation of the extinction coefficients of the SAA transients. When the stationary absorption band is normalized to the initial negative band (Fig. 3) the absorption coefficient of the depopulation band at 350 nm is equal to about 2300 M^{-1} cm^{-1}, while the stationary absorption coefficient for SAA is 23 000 M^{-1} cm^{-1} near this wavelength [18]. This means that about 10% of the molecules are transferred to the *trans*-keto tautomer, thus $c_P = 0.1c$, where c is the SAA concentration. Having this in mind, the fitted rate constants (Fig. 4) are $k_1 = 1.5 \times 10^3$ s^{-1} and $k_2 = 0.7 \times 10^9$ M^{-1} s^{-1} in ACN, while the parameter m is: $m = 0.82$ for $c = 5 \times 10^{-5}$ M, $m = 0.70$ for $c = 2.5 \times 10^{-5}$ M and $m = 0.50$ for $c = 1.1 \times 10^{-5}$ M.

For SAA in HEX the *trans*-keto tautomer decay kinetics is also well described by Eq. (1), however the fitted values of k_1 and k_2 are not constant for different concentrations. Since the decay is faster by approximately one order of magnitude than in ACN, a possible explanation is that the k_2 value is close to the diffusion rate constant in HEX at room temperature ($k_d = 8RT/3\eta = 2 \times 10$ 10 M^{-1} s^{-1}) and therefore, the reaction cannot be described by the simple second-order kinetics [32].

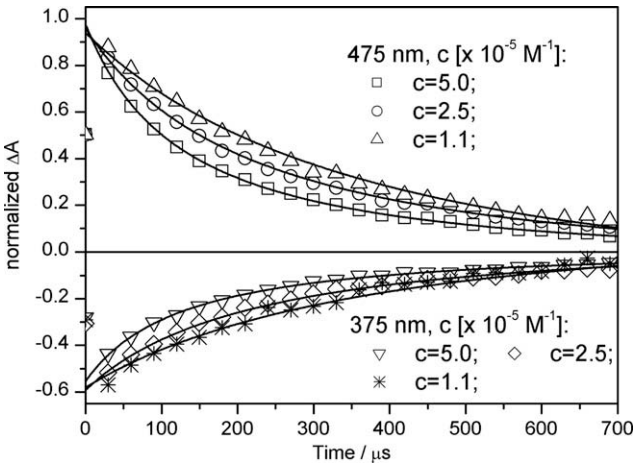

Fig. 4. Kinetic curves of the transient absorption signals of SAA in ACN for different concentration with the fitted function according to Eq. (1). The fitted rate constants are: $k_1 = 1.5 \times 10^3\ s^{-1}$ and $k_2 = 0.7 \times 10^9\ M^{-1}\ s^{-1}$. For clarity, only every 150 experimental point is shown.

On the contrary, in alcohols the *trans*-keto tautomer lifetime is significantly decreased as observed for some other Schiff bases [7,19], there is no influence on the SAA concentration and the decay is mono-exponential (time constants: 11 μs in TFE, 9 μs in MeOH and 0.15 μs in HFIP). This effect might be explained by the solvent assisted reenolization involving the complex with one or more solvent molecules, like proposed for salicylidene-1-naphtylamine [6]. More detailed studies of 2-(2′-hydroxyphenyl)-3-H-indole [33] indicated the participation of two alcohol molecules in the catalysis of the deactivation rate of *trans*-keto tautomer. By analogy with those studies, the back proton transfer in the SAA molecule probably takes place through the intermolecular exchange of the hydrogen atom from the alcohols' hydroxyl groups, see Fig. S14. Very short *trans*-keto tautomer lifetimes were also observed for SAA in the micelles: 0.45 μs in SDS, 0.25 μs in TX and 0.20 μs in CTAB (Fig. S10). This should be probably explained by the water-assisted process (water has proton donating ability comparable to that of strong alcohols – see Table S1) and confirms that the SAA is located in the polar part of the micelles, where the water molecules are present. The molecular size of SDS micelles is smaller than that of CTAB and TX ones [22,23] and the free volume for the deactivation mechanism is more restricted, therefore the SAA *trans*-keto tautomer lifetime might be longer in SDS. In alcohols and micelles an extra transient absorption feature with a maximum between 400 and 425 nm can be also recognized as an additional component of minor amplitude and lifetime in the range of single μs (Figs. S11 and S13). Its possible origin is the open *trans*-enol structure (with respect to C–C (phenyl) bond) created after reenolization, which then converts to the initial closed (with intramolecular hydrogen bond) enol tautomer.

Table 3
Summary of the main SAA tautomers' properties in solution and in micellar systems

Tautomers	SAA in solution	SAA in micelles
Enol	Stationary absorption band: red shift with increasing polarizability and blue shift with increasing polarity and proticity.	Stationary absorption band similar to that in polar solvents.
cis-Keto	The shortest lifetime in polar solvents, the lifetime increases with increasing polarizability, viscosity and proticity. Single-exponential fluorescence decay (except for highly viscous solvents).	Lifetime comparable or longer than that in highly viscous solvents. Multi-exponential fluorescence decay with wavelength-dependent amplitudes of emission.
trans-Keto	Non-exponential decay and concentration dependant lifetime in non-protic solvents – mixed first and second order processes. Lifetime increases with increasing polarity. Proticity of the solvents drastically shortens the lifetime and makes it pure first order.	Very short lifetime comparable to that in most protic alcohols (due to the effect of water present in micelles). Only first order process.

To summarize, it has been found that three depopulation routes are responsible for the deactivation of the ground state of the SAA *trans*-keto tautomer in solution: 'normal' first-order process via the ground state of *cis*-keto tautomer (back *trans–cis* isomerisation followed by back intramolecular proton transfer), second-order double proton transfer in the hydrogen-bonded complex of two *trans*-keto tautomers and pseudo first-order solvent-assisted reenolization via the intermolecular proton transfer. The last mechanism operates very efficiently in alcohols and micellar systems. The proposed deactivation scheme for SAA is also presented in Fig. S14.

4. Conclusions

The photochromic cycle of SAA as well as spectroscopic and photophysical properties of the SAA tautomers participating in this cycle has been investigated by means of the stationary and time-resolved UV–vis spectroscopy. The similarities and differences between the SAA dynamics in homogeneous solvents and micellar systems are summarized in Table 3. SAA can be proposed as a convenient probe for studying the properties of photochromic Schiff bases in heterogeneous environments due to a remarkable resistance to hydrolysis, a considerable stabilization of the primary enol form and a relatively simple deactivation scheme.

Acknowledgements

This work was performed under financial support of the Ministry of Science and Higher Education (MNiSW) Poland project N204 149 32/3777. Dynamic measurements were made at the Center for Ultrafast Laser Spectroscopy at the A. Mickiewicz University in Poznan, Poland. The authors gratefully acknowledge Dr. Jerzy Karolczak assistance with time-resolved fluorescence measurements and Dr. Gotard Burdzinski assistance with nanosecond transient absorption measurements. We also thank Dr. Krzysztof Dobek and Dr. Dariusz Komar for permission to use their fitting program for time-resolved emission data.

Appendix A. Supplementary material

Supplementary data associated with this article can be found, in the online version, at doi:10.1016/j.cplett.2008.09.030.

References

[1] T. Rosenfeld, M. Ottolenghi, A.Y. Meyer, Mol. Photochem. 5 (1973) 39.
[2] P.F. Barbara, P.M. Rentzepis, L.E. Brus, J. Am. Chem. Soc. 102 (1980) 2786.
[3] K. Kownacki, Ł. Kaczmarek, A. Grabowska, Chem. Phys. Lett. 210 (1993) 373.
[4] K. Kownacki, A. Mordzinski, R. Wilbrandt, A. Grabowska, Chem. Phys. Lett. 227 (1994) 270.
[5] R.S. Becker, C. Lenoble, A. Zein, J. Phys. Chem. 91 (1987) 3509.
[6] J.S. Stephan, A. Mordziński, C. Ríos Rodríguez, K.H. Grellmann, Chem. Phys. Lett. 229 (1994) 541.
[7] A. Ohshima, A. Momotake, T. Arai, Bull. Chem. Soc. Jpn. 79 (2006) 305.
[8] S. Mitra, N. Tamai, Phys. Chem. Chem. Phys. 5 (2003) 4647.
[9] M.I. Knyazhansky, A.V. Metelitsa, M.E. Kletskii, A.A. Millov, S.O. Besugliy, J. Mol. Struct. 526 (2000) 65.
[10] M. Irie, Chem. Rev. 100 (2000) 1683.
[11] M. Sliwa et al., Chem. Mater. 17 (2005) 4727.

[12] G. Arcovito, M. Bonamico, A. Domenicano, A. Vaciago, J. Chem. Soc. B (1969) 733.
[13] X. Xu, X. You, Z. Sun, X. Wang, H. Liu, Acta Cryst. C50 (1994) 1169.
[14] M.M. Abo Aly, Spectrochim. Acta A 55 (1999) 1711.
[15] M. Mijanuddin, W.S. Sheldrick, H. Mayer-Figge, M. Ali, N. Chattopadhyay, J. Mol. Struct. 693 (2004) 161.
[16] M. Bossa, A. Sgamellotti, F.A. Gianturco, J. Chem. Soc. B (1969) 742.
[17] K. Kownacki, Ph.D. Thesis (in Polish), Inst. of Phys. Chem. Polish Acad. Sci., Warsaw, 1994.
[18] M. Ziółek, J. Kubicki, A. Maciejewski, R. Naskręcki, A. Grabowska, Phys. Chem. Chem. Phys. 6 (2004) 4682.
[19] M. Ziółek, G. Burdziński, K. Filipczak, J. Karolczak, A. Maciejewski, Phys. Chem. Chem. Phys. 10 (2008) 1304.
[20] R.W. Taft, M.J. Kamlet, J. Am. Chem. Soc. 98 (1976) 2886.
[21] J. Catalán, Solvent effects based on pure solvent scales, in: G. Wypych (Ed.), Handbook of Solvents, ChemTec Publishing, Toronto, 2001, p. 583.
[22] A. Maciejewski, A. Jakubowska, E. Dutkiewicz, W. Augustyniak, J. Col. Int. Sci. 177 (1996) 528.
[23] A. Maciejewski, J. Kubicki, K. Dobek, J. Col. Int. Sci. 295 (2006) 255.
[24] M. Ziółek, J. Kubicki, A. Maciejewski, R. Naskręcki, A. Grabowska, J. Chem. Phys. 124 (2006) 124518.
[25] E. Hadjoudis, A. Rontoyianni, K. Ambroziak, T. Dziembowska, I.M. Mavridis, J. Photochem. Photobiol. A: Chem 162 (2004) 521.
[26] K.K. Chatterjee, N. Farrier, B.E. Douglas, J. Am. Chem. Soc. 85 (1963) 2919.
[27] I.R. Bellobono, G. Favini, J. Chem. Phys. 48 (1968) 5738.
[28] W. Al-Soufi, K.H. Grellmann, B. Nickel, Chem. Phys. Lett. 174 (1990) 609.
[29] P.-T. Chou, M.L. Martinez, S.L. Studer, Chem. Phys. Lett. 195 (1992) 586.
[30] D. Lavabre, V. Pimienta, G. Levy, J.C. Micheau, J. Phys. Chem. 97 (1993) 5321.
[31] R.V. Bensasson, J.-C. Gramain, J. Chem. Soc. Farad. Trans. 1 (76) (1980) 1801.
[32] T.R. Waite, J. Chem. Phys. 32 (1960) 21.
[33] J.S. Stephan, C. Ríos Rodríguez, K.H. Grellmann, K.A. Zachariasse, Chem. Phys. 186 (1994) 435.